





CUX1 and I κ B ζ (NFKBIZ) mediate the synergistic inflammatory response to TNF and IL-17A in stromal fibroblasts

Kamil Slowikowski^{a,b,c,d,e,1} , Hung N. Nguyen^{a,1}, Erika H. Noss^{a,2}, Daimon P. Simmons^{a,f}, Fumitaka Mizoguchi^g , Gerald F. M. Watts^a, Michael F. Gurish^a, Michael B. Brenner^{a,3,4}, and Soumya Raychaudhuri^{a,b,c,d,e,h,3,4}

^aDivision of Rheumatology, Inflammation, and Immunity, Brigham and Women's Hospital, Harvard Medical School, Boston, MA 02115; ^bDivision of Genetics, Brigham and Women's Hospital, Harvard Medical School, Boston, MA 02115; ^cBroad Institute of MIT and Harvard, Cambridge, MA 02142; ^dDepartment of Biomedical Informatics, Harvard Medical School, Boston, MA 02115; ^eCenter for Data Sciences, Brigham and Women's Hospital, Boston, MA 02115; ^fDepartment of Pathology, Brigham and Women's Hospital, Harvard Medical School, Boston, MA 02115; ^gDepartment of Rheumatology, Graduate School of Medical and Dental Sciences, Tokyo Medical and Dental University, 113-8519 Tokyo, Japan; and ^hCentre for Genetics and Genomics Versus Arthritis, Manchester Academic Health Science Centre, University of Manchester, M13 9PL Manchester, United Kingdom

Contributed by Michael B. Brenner, January 3, 2020 (sent for review July 25, 2019; reviewed by Caroline Ospelt and Matthew Weirauch)

The role of stromal fibroblasts in chronic inflammation is unfolding. In rheumatoid arthritis, leukocyte-derived cytokines TNF and IL-17A work together, activating fibroblasts to become a dominant source of the hallmark cytokine IL-6. However, IL-17A alone has minimal effect on fibroblasts. To identify key mediators of the synergistic response to TNF and IL-17A in human synovial fibroblasts, we performed time series, dose-response, and gene-silencing transcriptomics experiments. Here we show that in combination with TNF, IL-17A selectively induces a specific set of genes mediated by factors including cut-like homeobox 1 (CUX1) and I κ B ζ (NFKBIZ). In the promoters of *CXCL1*, *CXCL2*, and *CXCL3*, we found a putative CUX1-NF- κ B binding motif not found elsewhere in the genome. CUX1 and NF- κ B p65 mediate transcription of these genes independent of LIFR, STAT3, STAT4, and ELF3. Transcription of *NFKBIZ*, encoding the atypical I κ B factor I κ B ζ , is IL-17A dose-dependent, and I κ B ζ only mediates the transcriptional response to TNF and IL-17A, but not to TNF alone. In fibroblasts, IL-17A response depends on CUX1 and I κ B ζ to engage the NF- κ B complex to produce chemoattractants for neutrophil and monocyte recruitment.

inflammation | transcription | regulation | RNA-seq | time series

In rheumatoid arthritis (RA), stromal fibroblasts are key components of the hyperplastic and invasive synovial tissue that mediates joint destruction and bone resorption (1). IL-17A, a cytokine produced by CD4⁺ Th17 cells (2) and other cells (3), helps to perpetuate the vicious inflammatory cycle localized to the joint tissue and contributes to induction, progression, and chronicity of RA (4). Briefly, leukocyte-derived cytokines activate stromal cells to produce inflammatory cytokines and chemokines, such as IL-6, IL-8, CCL2 (5), and granulocyte macrophage-colony stimulating factor (GM-CSF or CSF2) (6). In turn, these stromal-derived cytokines attract more leukocytes to infiltrate the synovial tissue and activate them to produce more cytokines. The infiltrating leukocytes produce tumor necrosis factor (TNF- α) and IL-17A, which synergizes with TNF to amplify the molecular pathways underlying chronic inflammatory disease pathogenesis (3).

The combination of TNF and IL-17A synergistically activates synovial fibroblasts to produce IL-6 (5), and these cells are a dominant source of IL-6 in the joint tissue (7, 8). While many cytokines are involved in RA, clinical efficacy of targeting TNF and IL-6 has clearly established their pivotal roles in pathogenesis (9). Clinical relevance of the synergistic activity of TNF and IL-17A has been supported by the observation that levels of TNF and IL-17A mRNA in RA synovial tissue predict early joint damage progression by magnetic resonance imaging (10). Joint damage progresses as TNF and IL-17A induce synovial fibroblasts to produce matrix metalloproteinases (MMPs) for digesting

extracellular matrix and invading the cartilage (11). Further, IL-17A plays a role in differentiation of osteoclast progenitors into bone-resorbing osteoclasts via increased expression of RANKL in osteoblasts (12).

However, most studies of transcriptional response to IL-17A have used qPCR to measure only the genes with known roles in the context of inflammation, osteoclastogenesis, angiogenesis, or neutrophil recruitment (5, 11, 13–18). One study used microarrays to measure genome-wide gene-expression response in a

Significance

Rheumatoid arthritis is characterized by elevated levels of inflammatory cytokines including TNF and IL-17A. Synovial fibroblasts produce inflammatory factors such as IL-6 in response to TNF, and the addition of IL-17A synergistically amplifies this response. We profiled the transcriptomic response of synovial fibroblasts to TNF and different IL-17A dosages over time, and defined a set of genes induced by the addition of IL-17A. We found that CUX1 and I κ B ζ (NFKBIZ) mediate leukocyte recruitment by regulating production of multiple cytokines and chemokines. We show that gene targets of CUX1 are elevated in synovial tissue from individuals with rheumatoid arthritis relative to controls. While many studies have focused on leukocytes, our results highlight CUX1 and I κ B ζ as key regulators of inflammation in synovial fibroblasts.

Author contributions: K.S., H.N.N., M.B.B., and S.R. designed research; K.S., H.N.N., E.H.N., D.P.S., F.M., G.F.M.W., and M.F.G. performed research; K.S., H.N.N., E.H.N., D.P.S., F.M., and G.F.M.W. contributed new reagents/analytic tools; K.S. analyzed data; and K.S., H.N.N., and S.R. wrote the paper.

Reviewers: C.O., University Hospital of Zurich; and M.W., Cincinnati Children's Hospital Medical Center.

The authors declare no competing interest.

Published under the PNAS license.

Data deposition: Microarray Data 1, Microarray Data 2, RNA-seq Data 1, and RNA-seq Data 2 have been deposited in the Gene Expression Omnibus (GEO) database, <https://www.ncbi.nlm.nih.gov/geo> (accession no. GSE129488). We have created an open-source interactive website to provide readers with a browser for the RNA-seq data, available at: <https://immunogenomics.io/fibrotome>. The source code for reproducing the analyses is available at <https://github.com/slowkow/fibrotome> and has been deposited to Zenodo at <https://doi.org/10.5281/zenodo.3647205>.

¹K.S. and H.N.N. contributed equally to this work.

²Present address: Division of Rheumatology, University of Washington, Seattle, WA 98109.

³M.B.B. and S.R. contributed equally to this work.

⁴To whom correspondence may be addressed. Email: mbrenner@research.bwh.harvard.edu or soumya@broadinstitute.org.

This article contains supporting information online at <https://www.pnas.org/lookup/suppl/doi:10.1073/pnas.1912702117/-DCSupplemental>.

First published February 20, 2020.

single sample 12 h after stimulation with IL-17A and IL-17F alone or in combination with TNF (5). An expanded view with robust measurements of transcriptional dynamics over time would help to reveal mediators in regulatory pathways downstream of TNF and IL-17A. While these regulatory pathways have been studied in leukocytes (19), there remains much to be learned about the transcriptional regulation of inflammatory functions in mesenchymal cells, such as synovial fibroblasts. For example, we recently described an autocrine loop driving IL-6 production that is only used by fibroblasts, and not by leukocytes, involving leukemia inhibitory factor (LIF), LIF receptor (LIFR), and signal transducer and activator of transcription 4 (STAT4) (7). Many different cell types have been shown to use the NF- κ B signaling pathway for inflammatory response, but additional components of this pathway are being discovered that modulate cell-type and condition-specific responses to inflammatory signals (20).

Surprisingly, IL-17A in the absence of TNF has a minimal transcriptional effect in fibroblasts, and defining its role with TNF requires a highly sensitive study. To identify key mediators of the response to TNF and IL-17A in human synovial fibroblasts, we use transcriptomics data from a high-resolution time series with multiple IL-17A doses. By measuring the in vitro transcriptomic effects caused by stimulation with TNF or costimulation with TNF and IL-17A at three doses of IL-17A (0, 1, 10 ng/mL), we identify genes with transcriptional changes proportional to IL-17A dose. We also find that transcription of specific sets of chemokines is controlled by different mediators. A molecular complex of NF- κ B p65 and cut-like homeobox 1 (CUX1) mediates transcription of CXC chemokines (*CXCL1*, *CXCL2*, *CXCL3*, *CXCL6*). In contrast, LIFR mediates transcription of CC chemokines (*CCL7*, *CCL8*, *CCL20*). We distinguish these transcriptional responses by silencing each mediator with short-interfering RNAs (siRNAs) and then assaying the downstream effects with RNA sequencing (RNA-seq). Furthermore, we find that transcription of the atypical I κ B factor I κ B ζ (NFKBIZ) is proportional to IL-17A dose, and I κ B ζ mediates IL-6, IL-8, and MMP-3 production only after costimulation with TNF and IL-17A, but not after TNF alone. Finally, we demonstrate that fibroblasts require these mediators to recruit neutrophils and monocytes in an in vitro assay.

Results

TNF and IL-17A Synergistically Activate IL-6 and MMP-3 Production.

To demonstrate the synergy between TNF and IL-17A, we stimulated synovial fibroblasts with 16 combinations of dosages of TNF (0, 0.1, 1, 10 ng/mL) and IL-17A (0, 1, 10, 100 ng/mL). We cultured primary fibroblasts from two RA donors and measured IL-6 protein levels in the supernatant, stimulated the cells, by ELISA. Stimulation with one cytokine (TNF or IL-17A) is significantly less effective at inducing IL-6 than costimulation with TNF and IL-17A. We saw 1.2 ng/mL IL-6 after stimulation with IL-17A alone (100 ng/mL), and 2.6 ng/mL IL-6 after TNF alone (10 ng/mL) (Fig. 1A). In contrast, we saw 49.3 ng/mL of IL-6 in the supernatant after costimulation with TNF (10 ng/mL) and IL-17A (100 ng/mL); the addition of IL-17A caused a 20-fold increase in IL-6 levels relative to stimulation with TNF alone (Fig. 1A). MMP-3 protein levels showed a similar synergistic response to TNF and IL-17A (Fig. 1A). These results confirm previous reports that TNF and IL-17A synergistically activate IL-6, MMP-3, and other inflammatory cytokines (11, 13–16, 18).

IL-17A Requires TNF to Induce a Gene-Expression Response in Fibroblasts.

Since TNF and IL-17A induce synergistic protein production of IL-6 and MMP-3, we decided to assay the direct genome-wide transcriptional effects of IL-17A. To do this, we conducted two initial transcriptomics experiments after stimulation with IL-17A or TNF, alone or in combination.

First, we profiled one synovial fibroblast cell line at nine time points over 72 h in four different conditions: Media only, TNF (1 ng/mL), IL-17A (1 ng/mL), and TNF with IL-17A (1 ng/mL and 1 ng/mL). We used microarrays to assay the transcriptional response (Microarray Data 1) (*SI Appendix*, Fig. S1A and Dataset S1). After stringent quality control, we fit a linear model to each gene to find which genes show differential expression between conditions (*Methods*). In response to IL-17A alone, three genes (*NFKBIZ*, *TNFAIP6*, and *CXCL1*) were differentially expressed relative to media (fold-change [FC] > 1.5 and false-discovery rate [FDR] < 0.05) (*SI Appendix*, Fig. S1F). On the other hand, 1,208 genes responded to TNF alone (*SI Appendix*, Fig. S1G). In response to TNF and IL-17A, 15 genes were differentially expressed relative to TNF alone (*SI Appendix*, Fig. S1H). We also applied principal component analysis (PCA) (21) to Microarray Data 1. Along the first two components, samples stimulated with IL-17A alone are most similar to unstimulated samples, and there is little difference between samples stimulated with TNF alone or TNF and IL-17A (*SI Appendix*, Fig. S1B and C). We conclude that IL-17A is dependent on the presence of TNF to induce significant effects on gene expression, consistent with our ELISA results for protein levels of IL-6 and MMP-3 (Fig. 1A).

Given the subtle transcriptional difference between costimulation with TNF and IL-17A versus TNF alone, we ran a second experiment where we assayed gene-expression response in four synovial fibroblast cell lines (two RA and two osteoarthritis [OA]) 24 h after stimulation (Microarray Data 2 GSE93720) (*SI Appendix*, Fig. S1D and Dataset S2). This experiment replicated the differential expression signal between TNF and IL-17A versus TNF from Microarray Data 1 ($r = 0.67$, $P < 10^{-15}$) (*SI Appendix*, Fig. S1E). This gave us confidence that a well-powered transcriptomics study could help to identify the downstream mediators that respond to costimulation with TNF and IL-17A.

Defining the Transcriptional Response to TNF and IL-17A in Fibroblasts with a High-Resolution Time Series and Dose-Response Study.

We used RNA-seq to assay transcriptomes of seven synovial fibroblast cell lines (four RA, three OA) at nine time points over 24 h after stimulation with TNF (1 ng/mL) and IL-17A (0, 1, and 10 ng/mL), resulting in a total of 175 RNA-seq profiles (*Methods* and Fig. 1B). By using RA and OA cell lines, we could look for responses consistent across tissue states. By using multiple IL-17A dosages, we could identify genes with expression proportional to IL-17A dose. By modeling the dynamics of each gene over time, we increased our statistical power to identify differentially expressed genes (*Methods*). To view the results for any specific genes of interest, readers can visit <https://immunogenomics.io/fibrotime>, where all of the RNA-seq data are explorable in an interactive website.

Broadly, we found that genes could be subdivided into categories based on their response to TNF and IL-17A. We used linear models to estimate the effect sizes for each gene (*Methods* and Dataset S3). Next, we identified the genes with greatest response to 1) TNF at 6 h vs. 0 h and 2) costimulation with TNF and IL-17A vs. TNF alone (Fig. 1D). We limited our analysis to the 636 statistically significant genes (absolute FC > 2 and FDR < 0.05) and subdivided them into 5 categories (Fig. 1D). We also applied PCA (21) to these 636 genes (Fig. 1C), and found that the first component (explaining 31% of the total variance) identifies genes with strong activation or deactivation over time in response to TNF stimulation. The second (15% of variance) and third (14% of variance) PCs identify genes with expression altered by IL-17A dose.

Transcriptional Response Reveals Genes Selectively Induced by TNF and IL-17A Costimulation or TNF Alone. We defined category C1 as the set of genes induced by costimulation with TNF and IL-17A, but unchanged by TNF alone (Fig. 1D and F). C1 includes 26 genes

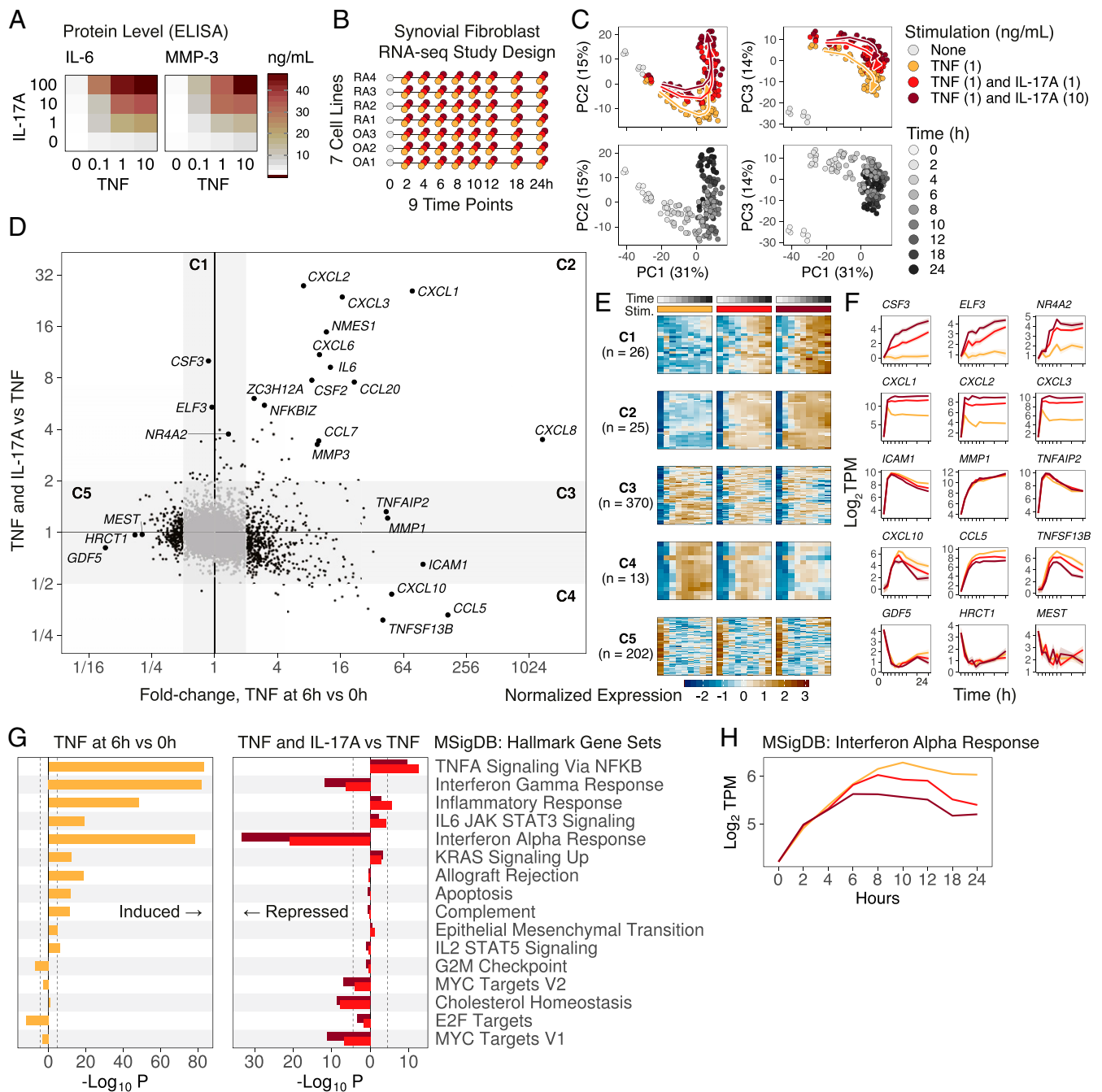


Fig. 1. Defining the transcriptional response to TNF and IL-17A in fibroblasts with a high-resolution time series and dose–response study. (A) Protein levels of IL-6 and MMP-3 measured by ELISA after stimulating with 16 different combinations of doses: TNF (0, 0.1, 1, 10 ng/mL) and IL-17A (0, 1, 10, 100 ng/mL). Costimulation with TNF and IL-17A results in synergistic IL-6 and MMP-3 protein production. (B) Our study design includes seven cell lines from patient tissues. We stimulated them with TNF (1 ng/mL) and three doses of IL-17A (0, 1, and 10 ng/mL). We measured gene expression at baseline and eight time points after stimulation. (C) PCA with 636 genes responsive to TNF alone or TNF and IL-17A. Samples fall along the principal curves. Sixty percent of the total variation is captured by the first three PCs. (D) Differential expression analysis shows that genes fall into five major categories, depending on the response to TNF alone (x axis) or to TNF and IL-17A (y axis). (E) Heatmaps with normalized expression for 636 genes, where rows are genes and columns are time points. From left to right, each heatmap shows response to TNF (1 ng/mL) and each of the three doses of IL-17A (0, 1, or 10 ng/mL). (F) Mean gene expression (lines) and SEM (ribbons) over time for genes with characteristic profiles: *CSF3*, *ELF3*, *NR4A2*, *CXCL1*, *CXCL2*, *CXCL3*, *ICAM1*, *MMP1*, *TNFAIP2*, *CXCL10*, *CCL5*, *TNFSF13B*, *GDF5*, *HRCT1*, *MEST*. (G) Gene set enrichment with MSigDB hallmark gene sets. The x axis shows signed *P* values indicating the strength of enrichment with induced or repressed genes for TNF at 6 h versus 0 h (Left) and TNF and IL-17A (1 or 10 ng/mL) versus TNF (Right). (H) We selected the 10 genes in the IFN Alpha Response gene set with the most significant *P* values for TNF and IL-17A (10 ng/mL) versus TNF, and show mean of the means of the 10 genes.

with dose-dependency on IL-17A such as *CSF3*, encoding G-CSF, a crucial factor for neutrophil survival and development (22, 23) (Fig. 1D and F, SI Appendix, Fig. S24, and Dataset S3). *IL11*, a cytokine

that is elevated in RA and promotes fibroblast invasion (24), was also transcribed in an IL-17A dose-dependent manner. The transcription factor (TF) with greatest expression response to IL-17A

was the epithelium-specific ETS factor encoded by *ELF3* (Fig. 1 D and F), so we hypothesized that ELF3 might mediate the IL-17A dose-dependent expression of other genes. For this reason, we included it in an siRNA gene-silencing experiment (see below). Another TF in category C1 is the orphan nuclear receptor encoded by *NR4A2*, which has been shown to induce synoviocyte proliferation and invasion (25), and also to directly control expression of *CXCL8* in inflammatory arthritis (26). Category C1 also includes “POU domain, class 2, transcription factor 2” encoded by *POU2F2*, a TF with a binding site motif in the promoters of *CSF3* and Ig genes (*SI Appendix*, Fig. S2A).

Category C2 has 25 genes induced by TNF and further induced by addition of IL-17A (Fig. 1 D–F), including members of the CXC subfamily of chemokines *CXCL1*, *CXCL2*, *CXCL3*, *CXCL6*, and *CXCL8*. Notably, *CXCL8* mRNA was 1,000-fold more abundant after TNF at 6 h relative to 0 h, and the other 4 chemokines were 17-fold more abundant on average (*SI Appendix*, Fig. S2B and Dataset S3). While TNF alone induced CXC chemokine transcription, the addition of IL-17A further increased transcription of these five chemokines in a dose-dependent manner (an additional 7-fold and 15-fold for 1 and 10 ng/mL IL-17A, respectively) (*SI Appendix*, Fig. S2B). We note that IL-8 (*CXCL8*), *CXCL1*, and *CXCL2* are potent neutrophil chemoattractants, complementing the function of G-CSF (encoded by *CSF3*) to promote neutrophil survival.

Category C3 genes are induced by TNF, but unaffected by the addition of IL-17A (Fig. 1 D–F). This is the largest category, with 370 genes, including TNF- α -induced genes *TNFAIP6* and *TNFAIP2*, as well as *MMP1* and bradykinin receptor (*BDKRB1*) (*SI Appendix*, Fig. S2C and Dataset S3). We tested Molecular Signatures Database (MSigDB) hallmark gene sets (27) for enrichment with TNF-responsive genes and found significant enrichments in the gene sets “TNFA signaling via NFkB,” “Interferon Alpha Response,” and “Interferon Gamma Response” (Fig. 1G).

Category C4 genes are induced by TNF, but transcription is dampened by the addition of IL-17A. C4 includes 13 genes related to interferon (IFN) response, such as *IRF1*, *IRF9*, *IFI30*, and *CXCL11* (*SI Appendix*, Figs. S2D and S3 A and B). Gene-set enrichment analysis shows that genes in the MSigDB hallmark gene set “Interferon Alpha Response” were induced by TNF, but repressed by the addition of IL-17A (Fig. 1G). Indeed, an increase from 1 ng/mL IL-17A to 10 ng/mL IL-17A causes more repression of these genes (Fig. 1H). This suggests that TNF activates—and IL-17A attenuates—the genes responsive to IFN- α .

Category C5 has 202 genes repressed by TNF but mostly unaffected by IL-17A. Enrichment with MSigDB hallmark pathways suggests that many of these genes are targets of E2F TFs involved

in cell cycle regulation, such as *STMN1*, *CDKN2C*, *CDC20*, *CDKN3*, *HMGB2*, *CDK1*, *CCNB2*, *CDC48*, and *TOP2A* (*SI Appendix*, Figs. S2E and S3 E and F). While TNF repressed these cell cycle-associated genes, it simultaneously induced transcription of genes involved in apoptosis such as *SOD2* and *BIRC3* (*SI Appendix*, Fig. S3 C and D). The genes most repressed by TNF include growth differentiation factor 5 (*GDF5*), histidine rich carboxyl terminus 1 (*HRCT1*), and mesoderm specific transcript (*MEST*) (Fig. 1D). For example, *GDF5*—a critical factor for normal synovial joint function (28) and synovial lining hyperplasia (29)—decreased 11-fold (FC 0.09, 95% CI 0.058 to 0.14, $P = 3e-20$) after 6 h of TNF relative to baseline.

We conclude that TNF alone is sufficient to activate transcription of the CXC subfamily of neutrophil recruitment chemokines (*CXCL1*, *CXCL2*, *CXCL6*, *CXCL8*) and monocyte recruitment chemokines (*CXCL3*, *CCL20*, *CCL7*), and that IL-17A synergizes with TNF to increase transcription of these chemokines. Costimulation with both TNF and IL-17A is required for transcription of the neutrophil survival factor G-CSF encoded by *CSF3*, while TNF alone is insufficient. Thus, costimulation of synovial fibroblasts with TNF and IL-17A activates a transcriptional program for recruiting neutrophils and monocytes and sustaining neutrophil survival.

TFs Underlying the Synergy between TNF and IL-17A. We used two strategies to find putative TFs that mediate the response to costimulation with TNF and IL-17A. First, we identified TFs with transcription proportional to IL-17A dose (categories C1 and C2), including *ELF3*, *POU2F2*, and *ZC3H12A*. Since *ELF3* expression increased (FC 5.4, 95% CI 4.4 to 6.6, $P = 2e-37$) after stimulation with IL-17A (10 ng/mL), we decided to study the global transcriptome-wide effects of silencing *ELF3* with siRNA.

Next, we searched for TF binding motifs in the promoters of differentially expressed genes. We used HOMER (30) to perform de novo motif enrichment analysis with 26 genes within categories C1 and C2 that had greater expression for 10 versus 1 ng/mL IL-17A (\log_2 FC > 1.5 [FC > 2.83] and FDR < 0.05) (*Methods*). As expected, we found motifs that closely resemble NF- κ B, REL, and JUND binding sites (Table 1). We also found a motif that might represent the binding site for CUX1, TCCGGATCGATC, that is present in the promoters of 4 of the 26 genes ($P = 1e-10$): *CXCL1*, *CXCL2*, *CXCL3*, *PIM2*. When we examined public CUX1 chromatin immunoprecipitation sequencing (ChIP-seq) data from ENCODE for three cell lines (GM12878, K562, MCF-7), we found evidence that CUX1 might bind these motifs. Consistent with our motif analysis and differential expression analysis, there are CUX1 ChIP-seq peaks in the promoters of *CXCL2*, *CXCL3*, *C15orf48* (*NMES1*), and *IL6*, as well as less than 5 kb upstream of the promoter of *CXCL6* (*SI*

Table 1. HOMER de novo motifs in gene promoters

Best match	P	FG (%)	BG (%)	Consensus	Promoters
NFkB-p65-Rel(RHD)/ThioMac-LPS-Expression(GSE23622)	10^{-12}	16	0.0043	CAGGGAATTTC	<i>CXCL1</i> , <i>CXCL2</i> , <i>CXCL3</i> , <i>CXCL6</i>
CUX1/MA0754.1/Jaspar	10^{-10}	16	0.016	TCCGGATCGATC	<i>CXCL1</i> , <i>CXCL2</i> , <i>CXCL3</i> , <i>PIM2</i>
Nur77(NR)/K562-NR4A1-ChIP-Seq(GSE31363)	10^{-10}	16	0.025	ACCTTYMCAWKA	<i>CCL20</i> , <i>CSF2</i> , <i>MMP3</i> , <i>TNFSF13B</i>
REL/MA0101.1/Jaspar	10^{-9}	20	0.11	TCCGGGTTTC	<i>CXCL1</i> , <i>CXCL2</i> , <i>CXCL3</i> , <i>NFKBIZ</i> , <i>PTGS2</i>
GLI2/MA0734.1/Jaspar	10^{-9}	16	0.027	GACCGCTGGC	<i>C15orf48</i> , <i>CD83</i> , <i>GOS2</i> , <i>IL411</i>
Hic1/MA0739.1/Jaspar	10^{-8}	24	0.51	GCGATGGCCC	<i>C15orf48</i> , <i>CCL20</i> , <i>CXCL1</i> , <i>CXCL2</i> , <i>CXCL3</i> , <i>GOS2</i> , <i>NFKBIZ</i>
EWSR1-FLI1/MA0149.1/Jaspar	10^{-7}	12	0.019	GAAGGAAGGCGA	<i>CXCL1</i> , <i>CXCL2</i> , <i>CXCL3</i>
JUND/MA0491.1/Jaspar	10^{-6}	20	0.56	GACTCATCCT	<i>CCL7</i> , <i>CSF2</i> , <i>IL11</i> , <i>MMP3</i> , <i>NFKBIZ</i>

HOMER de novo motif analysis of the promoters of 25 genes with statistically significant difference (\log_2 FC > 1.5 and FDR < 0.05) for 10 vs. 1 ng/mL of IL-17A. For each discovered motif, we show the name of a known motif that is similar to the newly discovered motif, the hypergeometric *P* value from HOMER, the percent of matches in the foreground (FG) set of 25 target sequences, the percent of matches in the background (BG) set of 39,486 sequences, and the list of genes in the foreground that have a match for the motif.

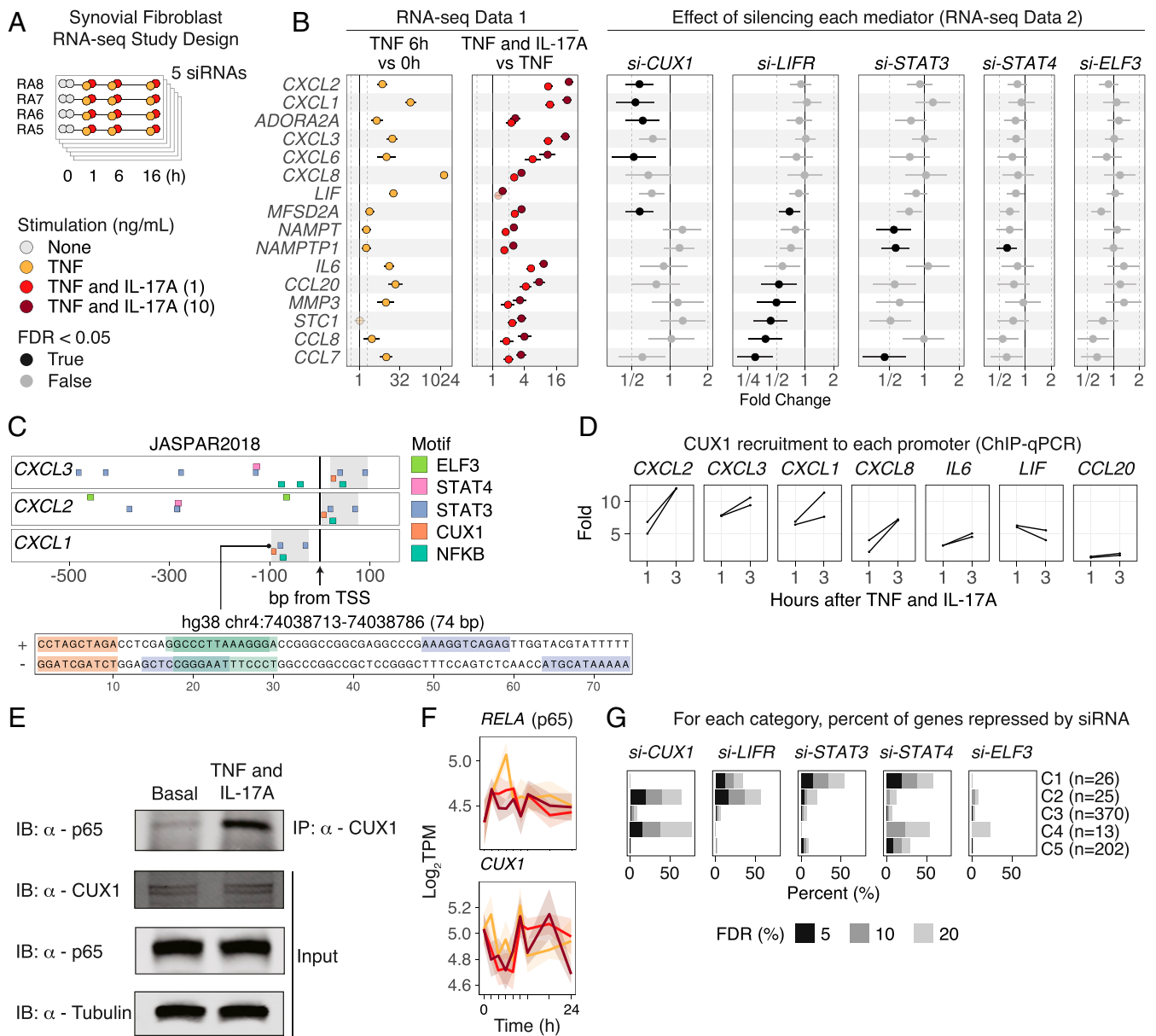


Fig. 2. CUX1 mediates transcription of *CXCL1*, *CXCL2*, *CXCL3*, independent of *LIFR*, *STAT3*, *STAT4*, and *ELF3*. (A) Our experimental design included four synovial fibroblast cell lines from patient tissues, four time points (0, 1, 6, and 16 h), two stimulations (TNF [0.1 ng/mL]; TNF [0.1 ng/mL] and IL-17A [1 ng/mL]), and five siRNAs (*CUX1*, *LIFR*, *STAT3*, *STAT4*, *ELF3*). (B) FC estimates and 95% CIs for 16 select genes that were responsive to IL-17A and were significantly repressed by at least one siRNA, or genes measured by ChIP-qPCR. *Left* two panels show stimulation effect estimates from RNA-seq Data 1, and *Right* five panels show siRNA effect estimates from RNA-seq Data 2. Dark color indicates FDR < 0.05. (C) The promoters of *CXCL1*, *CXCL2*, and *CXCL3* have a unique 74-bp sequence that contains motifs for CUX1 (GGATCGATC), NF- κ B (GCCCTTAAGGGA), and *STAT3* (AAAGGTCAGAG). (D) ChIP-qPCR of the CUX1 protein to seven gene promoters at three time points (0, 1, and 3 h) after costimulation with TNF and IL-17A. The y axis shows fold recruitment relative to the first time point (0 h), shown for two technical replicates. (E) After 4 h of stimulation with TNF (1 ng/mL) and IL-17A (1 ng/mL), NF- κ B p65 is detected in a pull-down of CUX1. (F) The mRNA levels of *RELA* (p65) and *CUX1* are insensitive to IL-17A, and are relatively stable over time. (G) For each of the five categories defined in Fig. 1, the percent of genes that are repressed (FC < 1.5 and FDR < 5%, 10%, and 20%) after silencing each mediator with siRNA.

Appendix, Fig. S4A). These results motivated us to assay the transcriptome-wide effects of silencing *CUX1*.

In addition to silencing *ELF3* and *CUX1*, we also decided to silence the genes encoding *LIFR* and *STAT4*. Previously, we found that *LIFR* and *STAT4* are key components of an autocrine loop controlling IL-6 production that is specific to fibroblasts and not leukocytes (7). We also decided to silence *STAT3* because it encodes a known mediator of inflammatory pathways (31), and we wanted to see how its function might be distinct from *STAT4* in the fibroblast response to inflammatory chemokines.

Transcriptomics Time Series after Silencing Putative Mediators. We selected five genes encoding putative mediators of IL-17A transcriptional effects (*ELF3*, *CUX1*, *LIFR*, *STAT3*, *STAT4*), silenced them with siRNAs, and assayed global gene expression with RNA-seq. We used qPCR to confirm that each of our selected siRNAs silences its intended target gene (SI Appendix, Fig. S5A). After incubating four RA synovial fibroblast cell lines with an siRNA for 2 d, we stimulated them with TNF (0.1 ng/mL) alone or TNF and IL-17A (1 ng/mL) and assayed the transcriptomes at four time points (0, 1, 6, and 16 h) (Fig. 2A). This experimental design let us

confirm that these putative mediators are acting downstream of IL-17A, and allows us to directly compare their transcriptional effects.

When we focus on the five categories of gene-expression response to TNF stimulation or TNF and IL-17 costimulation, we can see that silencing each mediator (*CUX1*, *LIFR*, *STAT3*, *STAT4*, *ELF3*) resulted in repression of genes in different categories (Fig. 2G), and that very few genes in category C3 (induced after TNF, no effect after IL-17A) were repressed after silencing these mediators. Furthermore, we clustered the 636 genes in categories C1, C2, C3, C4, and C5 into 15 patterns of gene expression with different profiles over time and IL-17A dose. We did this by using the Partitioning Algorithm based on Recursive Thresholding with Pearson distance and hierarchical clustering on the scaled expression data from RNA-seq Data 1 (32) (SI Appendix, Methods and Fig. S6A). Next, we looked at the intersection between the 15 patterns and genes significantly repressed ($FC < 1.5$ and $FDR < 0.05$) by each siRNA (SI Appendix, Fig. S6B). We found that each mediator controls different sets of genes with distinct expression profiles over time. We also looked at the intersection between these 15 patterns and the 5 categories we defined above (SI Appendix, Fig. S6C). For example, we found that two categories, C3 (induced by TNF, no effect from IL-17A) and C5 (repressed by TNF, no effect from IL-17A), could be subdivided into many different patterns over time. Finally, we tested each of the 15 patterns for enrichment in Reactome pathways (33), and found each pattern is enriched within different pathways (SI Appendix, Fig. S6D). For example, the genes in pattern 3 are activated by TNF, repressed by addition of IL-17A, and enriched in the reactome pathway called “Interferon Alpha Beta Signaling” (Fisher’s exact test $P < 10^{-25}$).

When we examined genes in categories C1 (induced only by costimulation) and C2 (induced by TNF, amplified by IL-17A), we found two distinct groups of genes with different responses to gene silencing (Fig. 2B). One group of genes was more repressed by silencing *CUX1*, and the other group was more repressed by silencing *LIFR*. Consistent with our motif analysis, silencing *CUX1* repressed category C2 genes *CXCL1*, *CXCL2*, *CXCL3*,

CXCL6, *CXCL8* (mean FC 0.60, 95% CI: 0.43 to 0.84). In contrast, these five genes were not strongly affected by silencing *ELF3*, *LIFR*, *STAT3*, or *STAT4* (mean FC 0.92, 95% CI: 0.66 to 1.3) (Fig. 2B). We validated this result by using qPCR to measure selected genes (*CCL7*, *CCL8*, *CCL20*, *IL6*, *CXCL1*, *CXCL2*, *CXCL3*) in the same cDNA libraries (SI Appendix, Fig. S5B). These data suggest at least two independent regulatory pathways for genes induced by costimulation with TNF and IL-17A.

CUX1 and NF- κ B p65 might form a molecular complex that binds a unique sequence in CXC gene promoters. In the JASPAR2018 database of genome-wide TF binding motif matches (34), we found a unique *CUX1*–NF- κ B nucleotide sequence motif in the promoters of *CXCL1*, *CXCL2*, and *CXCL3* (Fig. 2C). After a genome-wide BLAST search for the 74-bp sequence found in the promoter of *CXCL3* (hg38 chr4:74038713–74038786) that contains the *CUX1* and NF- κ B motifs, we found hits in four genomic locations: The promoters of *CXCL1*, *CXCL2*, *CXCL3*, and pseudogene *CXCL1P1* (SI Appendix, Fig. S4B). This replicates previous results showing that multiple CXC chemokines have both NF- κ B and *CUX1* binding sites in their promoters (35). Notably, this 74-bp sequence is identical to the promoter sequence in the mouse genome upstream of *Cxcl1* (chr5:90891066–90891295), suggesting that the same motif might be functional in mice. Next, we used ChIP-qPCR to test if *CUX1* binds selected promoters after stimulation with TNF and IL-17A. Indeed, *CUX1* recruitment to the promoters of *CXCL1*, *CXCL2*, and *CXCL3* increases more than 10-fold, on average, after 3 h of stimulation relative to baseline (Fig. 2D), and more than 6-fold, on average, after 1 h of stimulation (SI Appendix, Fig. S5H). Since *CUX1* binds the promoters of genes with the *CUX1*–NF- κ B motif, we hypothesized that *CUX1* might bind NF- κ B. Using an antibody against *CUX1*, we detected an increased amount of NF- κ B p65 in the pull-down fraction after stimulating fibroblasts with TNF and IL-17A (Fig. 2E). Using an antibody against p65, we detected an increasing amount of *CUX1* in the pull-down fractions 0.5 and 1 h after costimulation with TNF and IL-17A relative to no stimulation (SI Appendix, Fig. S5D), as well as an increased amount of

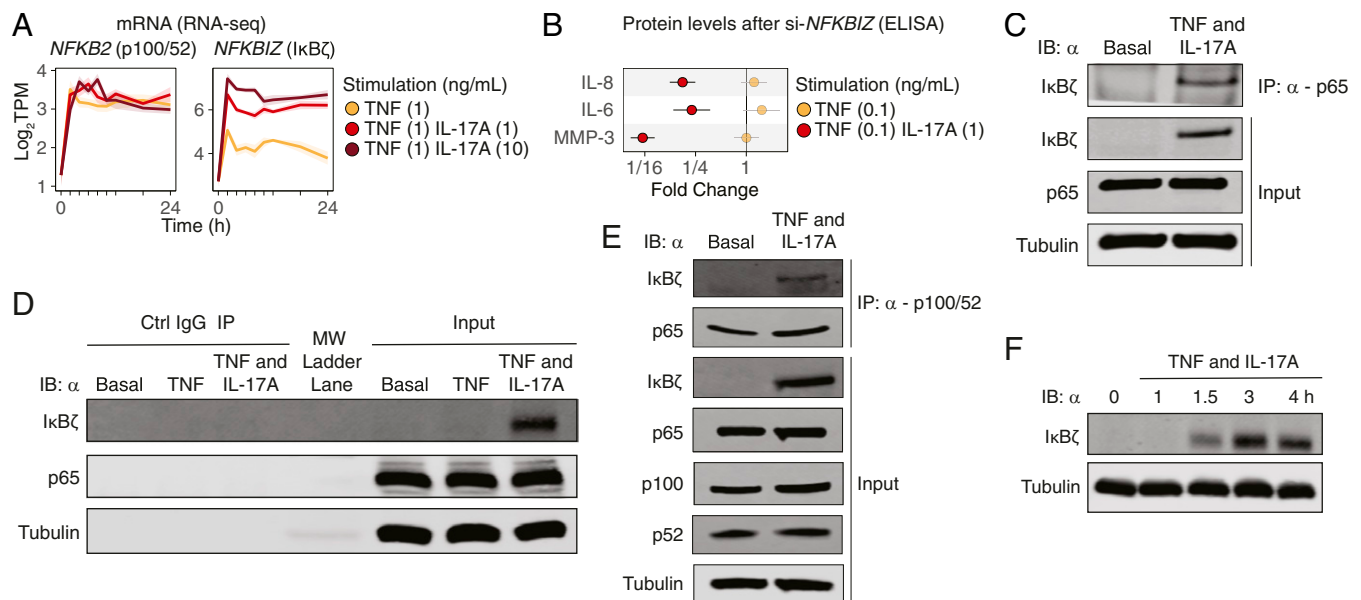


Fig. 3. $\text{IkB}\zeta$ binds NF- κ B p65 and p100/52, and mediates the response to TNF and IL-17A. (A) Gene expression of *NFKB2* (p100) and *NFKBIZ* ($\text{IkB}\zeta$) over time and IL-17A dosage in RNA-seq Data 1. The addition of IL-17 (10 ng/mL) increases transcription 5.5-fold ($P = 4e-59$) relative to TNF (1 ng/mL) alone. (B) Silencing *NFKBIZ* reduces protein levels of MMP-3, IL-6, and IL-8 after costimulation with TNF (0.1 ng/mL) and IL-17A (1 ng/mL), but not after stimulation with TNF alone. (C) $\text{IkB}\zeta$ is detected in a pull-down of NF- κ B p65. (D) $\text{IkB}\zeta$ is detected after costimulation with TNF and IL-17A, but not after TNF alone. (E) $\text{IkB}\zeta$ is detected in a pull-down of NF- κ B p100/52. (F) $\text{IkB}\zeta$ is detected 1.5 h or later after costimulation with TNF and IL-17A, but not after 1 h. IPs in C–E were performed after 4 h of costimulation with TNF (1 ng/mL) and IL-17A (1 ng/mL) or TNF alone (1 ng/mL).

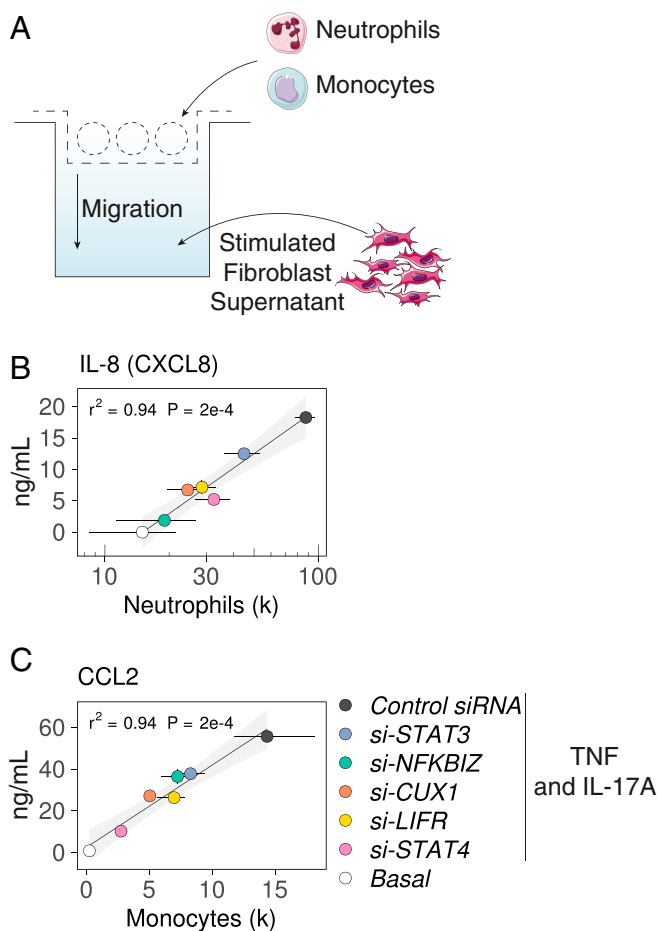


Fig. 4. CUX1 and IκBζ mediate neutrophil and monocyte recruitment in an in vitro migration assay. (A) We tested migration and protein levels in supernatant from synovial fibroblasts before stimulation (Basal) and 24 h after stimulation with TNF and IL-17A. (B) Silencing *CUX1* or *NFKBIZ* (IκBζ) reduces neutrophil recruitment. Neutrophil migration ($n = 2$) is correlated with protein level of IL-8 ($n = 2$) in the supernatant measured by ELISA. (C) Silencing *CUX1* or *STAT4* reduces monocyte recruitment ($n = 3$). Monocyte migration is correlated with protein level of CCL2 ($n = 2$) in the supernatant measured by ELISA. In B and C, dots represent mean; whiskers represent minimum and maximum.

CUX1 in the pull-down fraction after TNF and IL-17A relative to TNF alone (SI Appendix, Fig. S5E).

In contrast, we did not detect CUX1 in the pull-down fraction of p100/52 (SI Appendix, Fig. S5F). This is consistent with our observations of repressed transcription of *CXCL1*, *CXCL2*, and *CXCL3* only after silencing p65 but not after silencing p52 (SI Appendix, Fig. S5G). Notably, CUX1 does not require IκBζ to bind NF-κB p65, because CUX1 binds NF-κB p65 after TNF stimulation (SI Appendix, Fig. S5E) and 0.5 h after costimulation with TNF and IL-17A (SI Appendix, Fig. S5D), whereas IκBζ protein is not detected after TNF stimulation (Fig. 3D) and is not detected until 1.5 h after costimulation (Fig. 3F). Since mRNA levels of *RELA* (gene encoding NF-κB p65) and *CUX1* remain relatively constant over time (Fig. 2F) and protein levels do not seem to change with stimulation (Fig. 2E), these data suggest that CUX1 and NF-κB p65 might form a molecular complex. The CUX1–NF-κB–p65 complex becomes more abundant after stimulation with TNF, and even more abundant after costimulation with TNF and IL-17A (SI Appendix, Fig. S5D and E), so we hypothesize that complex formation may be mediated by posttranslational modifications. Then, this complex might bind the promoters of CXC

chemokines and induce transcription of these genes in synovial fibroblasts.

In addition to the group of genes repressed by silencing *CUX1*, a second group of genes was repressed after silencing *LIFR*. This includes the genes encoding C-C type chemokines encoded by *CCL8*, *CCL20*, as well as *MMP3* and *STC1* (Stanniocalcin-1) (mean FC 0.34, 95% CI: 0.22 to 0.51) (Fig. 2B). These four genes were unaffected after silencing *CUX1* (mean FC 1.0, 95% CI: 0.67 to 1.6), suggesting their transcription is not mediated by CUX1. *CCL8* (MCP-2) is a chemoattractant and activator of monocytes, whereas *CCL20* is a chemoattractant for lymphocytes and is known to recruit CCR6⁺ Th17 cells to sites of inflammation (36). Our data suggest that chemoattraction of leukocytes is a primary function of the response to TNF and IL-17A, and that this response involves at least two independent pathways mediated by CUX1 and LIFR.

IκBζ Binds NF-κB p65 and p100/52, and Mediates the Response to TNF and IL-17A. Since NF-κB is a known mediator of inflammatory pathways, and *NFKBIZ* transcription is proportional to IL-17A dose (Fig. 3A), we tested the effects of silencing *NFKBIZ*, the gene encoding IκBζ. We measured protein levels of IL-6, IL-8 (CXCL8), and MMP-3 after stimulating synovial fibroblasts with TNF alone or with the combination of TNF and IL-17A. Silencing *NFKBIZ* reduced protein levels of IL-6, IL-8, and MMP-3 after costimulation with TNF alone (Fig. 3B). Indeed, we did not detect IκBζ protein in unstimulated fibroblasts or in fibroblasts stimulated with TNF (Fig. 3D). Instead, we only detected IκBζ protein after costimulation with TNF and IL-17A (Fig. 3C–E). By testing multiple time points, we found that IκBζ protein is not detected 1 h after costimulation, but it is detected at 1.5 h (Fig. 3F). Next, we tested if IκBζ binds NF-κB to modulate the transcription of its downstream targets in fibroblasts. Using an antibody against NF-κB p65, we detected increased levels of IκBζ in the pull-down fraction after stimulating fibroblasts with TNF and IL-17A, relative to unstimulated fibroblasts (Fig. 3C). Furthermore, using an antibody against NF-κB p100/52 showed a similar result (Fig. 3E), indicating that IκBζ might form a complex with both p65 and p100/52.

CUX1 and IκBζ Mediate Neutrophil and Monocyte Recruitment. Neutrophils are the most abundant cells in the synovial fluid of inflamed joints in RA (37, 38), and abundance of synovial macrophages correlates with radiologic score of joint damage (39) and disease activity (40). Since fibroblasts could be an important source of chemoattractants in the synovium, we performed in vitro assays to test which mediators are required for recruitment of neutrophils and monocytes. Briefly, we stimulated synovial fibroblast cell lines with TNF and IL-17A for 24 h after silencing *CUX1*, *LIFR*, *STAT3*, *STAT4*, or *NFKBIZ*. Then, we tested the supernatants in a transwell migration experiment (Fig. 4A and Methods).

After silencing *CUX1* or *LIFR*, the supernatant from synovial fibroblasts was less effective at inducing migration of neutrophils (t test $P = 0.05$ and 0.06 , respectively) (Fig. 4B). The number of migrated cells was proportional to the protein level of IL-8 (CXCL8) in the supernatant, and silencing *NFKBIZ* had the greatest effect on neutrophil migration and IL-8 protein level. While monocyte migration was reduced after silencing of *CUX1* or *NFKBIZ* (t test $P = 0.04$ and 0.06 , respectively) (Fig. 4C), silencing *STAT4* had the greatest effect on monocyte migration and CCL2 protein level. We conclude that, in synovial fibroblasts, CUX1 and IκBζ mediate the production of chemoattractants necessary for the recruitment of neutrophils and monocytes.

Genes Induced by TNF and IL-17A Are Highly Expressed in RA Synovial Tissues. To test if genes induced by TNF or TNF and IL-17A are highly expressed in vivo, we examined public RNA-seq data from two large-scale transcriptomics studies that include inflamed RA

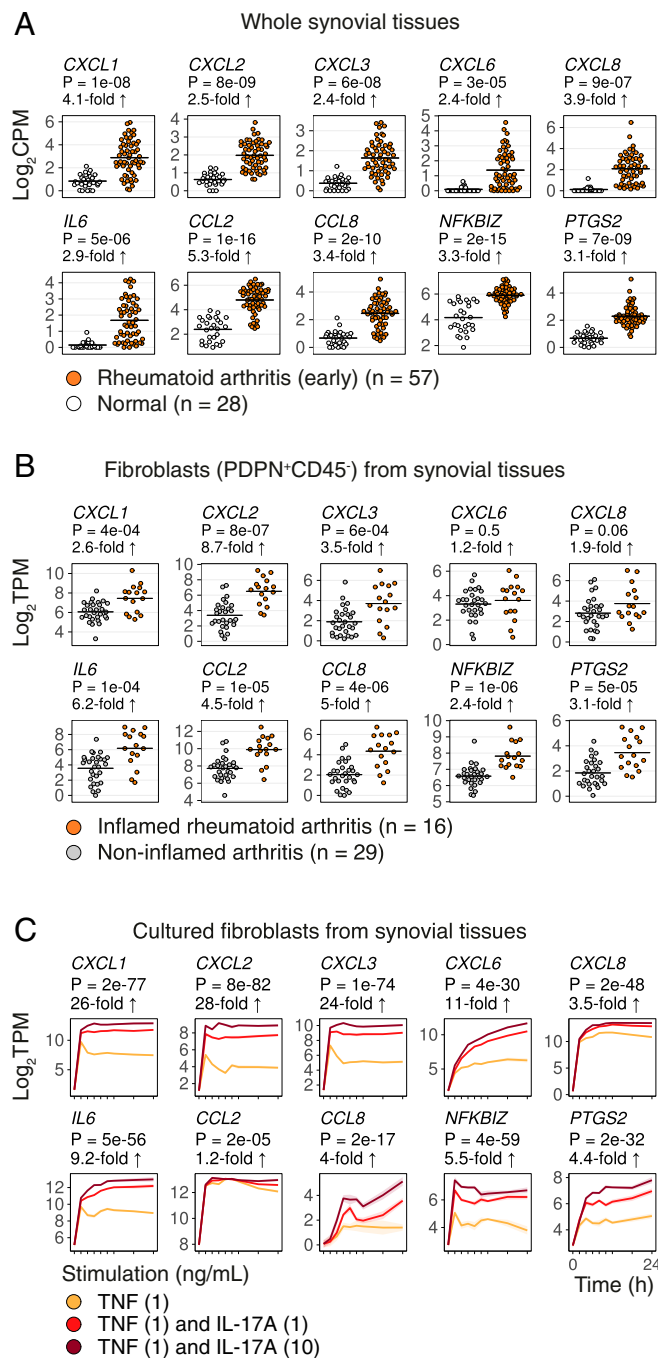


Fig. 5. Genes induced by TNF and IL-17A are highly expressed in RA synovial tissues. Transcript abundances from (A) RNA-seq data for whole synovial tissues (NCBI GEO GSE89408) or (B) RNA-seq data for sorted synovial fibroblasts (CD45⁺PDPN⁺) from synovial tissues (ImmPort 5DY998). Dots represent samples, lines represent means. FCs and *t* test *P* values. (C) Transcript abundances from RNA-seq Data 1 over time and IL-17A dose. FCs and *t* test *P* values for TNF (1 ng/mL) and IL-17A (10 ng/mL) versus TNF (1 ng/mL).

synovial tissues (8, 41). We focused on the 51 genes in categories C1 or C2 and tested for differential gene expression in each study. First, we compared 57 bulk synovial tissues (all cell types) from early RA versus 28 normal tissues (41) (Fig. 5A). Fourteen of 26 genes in category C1 and 20 of 25 genes in category C2 were higher in early RA, with $FDR < 0.05$. Since this study gave us a glimpse of the transcriptomic profile of the whole tissue, we next looked only at the contribution from fibroblasts. In the second study, sorted CD45⁺PDPN⁺

fibroblasts were isolated from synovial tissues, and here we compared 16 samples of fibroblasts from inflamed RA tissues versus 29 from noninflamed tissues (lower abundance of infiltrating leukocytes) (8) (Fig. 5B). Two of 26 genes in category C1 (*LYPD3* and *NR4A2*) and 9 of 25 genes in category C2 (including *CXCL1*, *CXCL2*, *CXCL3*, *NFKB1Z*) were higher in fibroblasts from inflamed RA than noninflamed arthritis tissues with $FDR < 0.05$. This suggests that synovial fibroblasts may be an important source of the chemokines encoded by *CXCL1*, *CXCL2*, *CXCL3*, *CXCL6*, *CXCL8*, *IL6*, *CCL2*, and *CCL8*. This also highlights the relevance of CUX1 and I κ B ζ as mediators of transcription in inflamed human tissue.

Discussion

We provide a genome-wide view of dynamic transcriptional responses to the combination of TNF and IL-17A and to TNF alone. Since IL-17A by itself has weak transcriptional effects, we used time-series transcriptomics after stimulation with TNF and three dosages of IL-17A (0, 1, 10 ng/mL), replicated across seven human donor-derived cell lines. Multiple dosages of IL-17A allowed us to confidently identify genes with transcriptional abundance proportional to IL-17A dosage. We defined categories of genes by looking at their transcriptional responses to TNF alone and costimulation with TNF and IL-17A. For example, many genes known to be transcriptionally induced by IFN- α and IFN- γ are induced by TNF alone but attenuated by the addition of IL-17A. By querying public RNA-seq data from in vivo samples, we also showed that many genes induced by TNF and IL-17A are more highly expressed in inflamed RA than normal synovial tissues, and in particular in synovial fibroblasts from RA joint tissues (Fig. 5).

TNF is known to induce fibroblasts to produce many inflammatory cytokines, and IL-17A has been shown to synergize with TNF to further induce key cytokines, such as IL-6 (13–16), neutrophil attracting chemokines (5, 17), and MMPs (11, 18). Two TFs, NF- κ B and C/EBP, control synergistic production of IL-6 (11, 15) in response to the combination of TNF and IL-17A. Since IL-17A receptor protein levels (*SI Appendix, Fig. S7 A–D*) and transcript levels (*SI Appendix, Fig. S7E*) are stable over time and IL-17A stimulation, we conclude that expression level of IL-17A receptors cannot explain the synergistic response to TNF and IL-17A. Instead, we believe that transcription, translation, and posttranslational modification of downstream mediators, such as CUX1 and I κ B ζ , are necessary to explain the increased inflammatory response induced by IL-17A in combination with TNF.

Among the list of IL-17A dose-responsive genes, we saw known IL-17A mediators such as *NFKB1Z* (42) and *ZC3H12A* (43). We used motif enrichment analysis to discover a unique CUX1–NF- κ B motif, predicted that CUX1 mediates transcription of CXC chemokines, and predicted that CUX1 might form a complex with NF- κ B. We validated these predictions by showing that silencing CUX1 with siRNA represses transcription of the genes with the CUX1–NF- κ B motif (*CXCL1*, *CXCL2*, *CXCL3*), and by showing that NF- κ B p65 binds CUX1 after costimulation with TNF and IL-17A. We found increased CUX1 binding to the promoters of *CXCL1*, *CXCL2*, and *CXCL3* after stimulation with TNF and IL-17A, suggesting that a CUX1–NF- κ B complex directly regulates transcription of these chemokines. Our data suggest that CUX1 mediated transcription is independent of LIFR, STAT3, STAT4, and ELF3, because silencing these mediators did not repress transcription of *CXCL1*, *CXCL2*, and *CXCL3*.

CUX1 is a homeobox TF with ubiquitous expression across mammals and essential roles in development and homeostasis (44), but its role in inflammation is not well understood. Previously, in tumor-associated macrophages, CUX1 was found to bind NF- κ B p65 and repress transcription of chemokines *CXCL10* and *CCL5* (45). Here, in fibroblasts, we find that the CUX1–NF- κ B–p65 complex induces chemokine transcription, suggesting cell-type-specific regulation. CUX1 has multiple protein isoforms

(46), but silencing *CUX1* mRNA appears to affect only the p200 isoform (*SI Appendix, Fig. S5C*), suggesting that CUX1 p200 is the dominant isoform in fibroblasts. In future studies, we might expect to find that additional homeobox TFs work with NF- κ B to regulate inflammation, with different cell-type-specific effects.

Previously, I κ B ζ , a unique member of the I κ B family with a distinct role as a coactivator of NF- κ B, was shown to be induced in macrophages after stimulation with a number of different Toll-like receptor ligands and IL-1 β , but not after stimulation with TNF alone (47). I κ B ζ regulates transcription of a specific set of genes such as *Csf3* in mouse embryonic fibroblasts (48). Here, we found that I κ B ζ is one of the critical mediators for the synergistic response to TNF and IL-17A in fibroblasts. Silencing *NFKBIZ* (the gene encoding I κ B ζ) reduced production of IL-6 and MMP3 after costimulation with TNF and IL-17A, but had no effect after stimulation with TNF alone (Fig. 3B). We also found that synovial fibroblasts require I κ B ζ for transcription of *CXCL8*, for production of the encoded protein IL-8, and for recruitment of neutrophils in vitro. Thus, I κ B ζ has a critical role in the inflammation caused by activated fibroblasts.

IL-17A is an important cytokine in autoimmune and inflammatory diseases (49, 50), such as psoriasis, psoriatic arthritis, ankylosing spondylitis, RA (19), inflammatory bowel disease, and multiple sclerosis (51). Clinical trials have led to the approval of two antibodies targeting IL-17A for treatment of psoriasis: Secukinumab is approved for psoriasis, psoriatic arthritis, and ankylosing spondylitis (52); and ixekizumab is approved for psoriasis (53). One might have expected similar results for RA, since IL-17A knockout suppresses arthritis in a collagen-induced arthritis mouse model (54), and mouse models have shown IL-17A involvement in all stages of RA (4). However, clinical trials of IL-17A inhibitors with RA patients have shown mixed results (55). In an ideal study, we would simultaneously measure protein levels of IL-17A in inflamed tissue samples along with transcriptomics to assess if a subset of patient samples with high IL-17A protein levels have a distinct gene-expression signature. Our results from this study suggest the potential for a personalized strategy to therapy: Perhaps the subset of patients where the distinct IL-17A downstream transcriptional effector program is observed is precisely the subset of patients where we might expect a clinical response to IL-17A blockade.

Methods

Cell Lines and Reagents. Human synovial fibroblasts were isolated as previously described (56) from tissues discarded and deidentified after synovectomy or joint replacement surgery. Each line was derived from a unique donor and used experimentally between passages 5 and 8. Cells were maintained in DMEM (Gibco) supplemented with 10% FBS (Gemini), 2 mM L-glutamine, 50 μ M 2-mercaptoethanol, antibiotics (penicillin and streptomycin), and essential and nonessential amino acids (Life Technologies). The following antibodies were used: anti-CUX1 (EMD Millipore); anti-p100/p52, anti-I κ B ζ (Cell Signaling Technology); anti-p65 (Santa-Cruz); anti- β -tubulin (Sigma); anti-CD45, anti-CD11b, anti-CD66b, (BioLegend); anti-CD14 (eBioscience). Other reagents were purchased from the following vendors: IL-6, IL-8, CCL2, and MMP3 ELISA kits, TNF, IL-17A (R&D Systems). All siRNAs (Silencer Select) were purchased from Life Technologies.

Immunoprecipitation. Total cell lysates were collected by washing cells once with cold PBS followed by addition of lysis buffer [50 mM Hepes pH 7.5, 5% glycerol, 100 mM NaCl, 0.25% Triton X-100, supplemented with a protease inhibitor mixture (Roche)] and phosphatase inhibitors (sodium orthovanadate, sodium fluoride, and β -glycerol phosphate). Cells were lysed for 30 min on ice followed by centrifugation at 15,000 rpm for 15 min at 4 $^{\circ}$ C. IP was done overnight at 4 $^{\circ}$ C using Protein A resins together with a rabbit antibody against the relevant target.

Quantitative Real-Time PCR. mRNA samples were extracted from cells using an RNeasy Micro Kit (Qiagen). cDNA synthesis was carried out using the QuantiTect Reverse Transcription Kit (Qiagen). qPCR reactions were performed in duplicate using the Brilliant III Ultra-Fast SYBR reagent (Agilent). qPCR primers are listed in [Dataset S5](#). Relative transcription level was calculated by using the $\Delta\Delta$ Ct method with GAPDH as the normalization control.

Fold induction was calculated by dividing the normalized mRNA at a certain time point with that at time 0 h. FC is the ratio of the normalized mRNA from cells expressing a specific siRNA vs. control (Ctrl) siRNA.

ChIP Assays. Fibroblasts were stimulated with TNF (1 ng/mL) + IL-17A (1 ng/mL) for different durations of time as indicated, followed by fixation with formaldehyde (1% final concentration) for 10 min. Cells were lysed in swelling buffer for 15 min (25 mM Hepes pH 7.8, 1.5 mM MgCl₂, 10 mM KCl, 0.1% Nonidet P-40, 1 mM DTT, protease inhibitor mixture) then in sonication buffer (50 mM Hepes pH 7.8, 140 mM NaCl, 1 mM EDTA, 0.1% SDS, 1% Triton X-100 supplemented with protease inhibitor mixture). Samples were sonicated for 2 min with 20-s pulse intervals and 1 min off at each interval at 4 $^{\circ}$ C using a Qsonica sonicator set at 28% output. Chromatin was immunoprecipitated using Dynabead Protein A resins (Life Technologies) together with a rabbit antibody against the relevant target at 4 $^{\circ}$ C overnight. DNA was purified using the phenol/chloroform precipitation method. The amount of DNA precipitated was quantified using qPCR. Fold recruitment was calculated by dividing the amount of ChIP DNA at indicated time points (normalized with input DNA) with that at 0 h (normalized with input DNA). ChIP primers are listed in [Dataset S5](#).

Western Blotting. Total cell lysates were collected by washing cells once with cold PBS followed by addition of lysis buffer (50 mM Hepes pH 7.5, 10% glycerol, 100 mM NaCl, 0.1% SDS, 1% Nonidet P-40, supplemented with protease inhibitors and phosphatase inhibitors sodium orthovanadate, sodium fluoride, and β -glycerol phosphate). Cells were lysed for 30 min on ice followed by centrifugation at 15,000 rpm for 15 min at 4 $^{\circ}$ C. Protein concentration was measured by the microBCA kit (Pierce). Equal amounts of total protein (~20 μ g per lane) were separated on an 8% SDS/PAGE gel. Proteins were transferred onto a PVDF membrane and blocked with 5% BSA in PBS and probed with primary antibodies overnight at 4 $^{\circ}$ C, followed by secondary antibodies conjugated with IRDye 680 or 800 (Rockland). Membranes were scanned with a Li-COR Odyssey scanner.

Leukocyte Migration. Fibroblasts were transfected with a control siRNA, or siRNA against a gene by reverse transfection using the RNAiMax reagent (Life Technologies) on day 1. The following day, cells were switched to 0.5% serum media and after 24 h they were stimulated with TNF (0.5 ng/mL) + IL-17A (0.5 ng/mL) for another 24 h before supernatants were collected and added to the bottom well of a 24-well plate. Neutrophils (PMNs) purified from blood using the neutrophil isolation kit (Stem Cell Technologies) and peripheral blood mononuclear cells (PBMC) containing monocytes purified from blood using Ficoll isolation technique were then introduced to the top well (Corning, 3- μ m pores insert) at the concentration of 1 million 1×10^6 cells/mL for PMNs and 2×10^6 cells/mL for PBMC. After 75 min (PMN migration) or 3 h (monocyte migration), cells from the bottom well were collected and the number of neutrophils, monocytes recruited toward the bottom well were quantified by flow cytometry using (anti-CD66b and anti-CD11b for neutrophils; anti-CD14 and anti-CD45 for monocytes), and cell numbers were normalized using counting beads (Spherotech).

RNA-Seq Expression Profiling. Fibroblasts were plated on day 1 at 50,000 cells per well in 24-well plates in 10% FBS containing media. Cells were serum-starved on day 2 by changing to 1% FBS-containing media. Cells were either left unstimulated or stimulated with TNF (1 ng/mL) or TNF (1 ng/mL) + IL-17A (1 ng/mL) for various durations of time. Samples were collected and RNA was extracted using the RNeasy Micro Kit (Qiagen). RNA-seq libraries were prepared with the Smart-Seq2 protocol.

siRNA Silencing. Fibroblasts were transfected with an siRNA by reverse transfection at 30 nM using the RNAi Max reagent (Life Technologies) in 10% FBS containing media. Cells were then switched to serum-starving media containing 1% FBS on day 2. Cells were stimulated as indicated on day 3. Efficiency of siRNA silencing was assessed by qPCR (*SI Appendix, Fig. S5A*).

Microarray Data Analysis. We normalized the microarray expression data with the robust multiarray averaging algorithm (57), assessed the quality of each array, and fit linear models with the limma R package (58) to test for differential gene expression (*SI Appendix, Methods*).

RNA-Seq Data Analysis. We used kallisto (v0.43.1) (59) to quantify transcripts per million (TPM) for all of the transcripts reported in Ensembl release 89 (60). To get TPM for each gene, we added the TPM values for all of the transcripts that belong to a gene. We used limma R package (58) to test for differential gene expression and to test for enrichment with gene sets from MSigDB (27) (*SI Appendix, Methods*).

Data Availability. Microarray Data 1, Microarray Data 2, RNA-seq Data 1, and RNA-seq Data 2 are available at the National Center for Biotechnology Information Gene Expression Omnibus accession no. GSE129488. We created an open-source interactive website to provide readers with a browser for the RNA-seq data, available at <https://immunogenomics.io/fibrotome>. Source code for the website and for reproducing our analyses is available at <https://github.com/slowkow/fibrotome> and has been deposited to Zenodo at <https://doi.org/10.5281/zenodo.3647205>.

1. N. Bottini, G. S. Firestein, Duality of fibroblast-like synoviocytes in RA: Passive responders and imprinted aggressors. *Nat. Rev. Rheumatol.* **9**, 24–33 (2013).
2. M. Chabaud *et al.*, Human interleukin-17: A T cell-derived proinflammatory cytokine produced by the rheumatoid synovium. *Arthritis Rheum.* **42**, 963–970 (1999).
3. L. Monin, S. L. Gaffen, Interleukin 17 family cytokines: Signaling mechanisms, biological activities, and therapeutic implications. *Cold Spring Harb. Perspect. Biol.* **10**, a028522 (2018).
4. G. Benedetti, P. Miossec, Interleukin 17 contributes to the chronicity of inflammatory diseases such as rheumatoid arthritis. *Eur. J. Immunol.* **44**, 339–347 (2014).
5. S. Zrioual *et al.*, Genome-wide comparison between IL-17A- and IL-17F-induced effects in human rheumatoid arthritis synoviocytes. *J. Immunol.* **182**, 3112–3120 (2009).
6. K. Hirota *et al.*, Autoimmune Th17 cells induced synovial stromal and innate lymphoid cell secretion of the cytokine GM-CSF to initiate and augment autoimmune arthritis. *Immunity* **48**, 1220–1232.e5 (2018).
7. H. N. Nguyen *et al.*, Autocrine loop involving IL-6 family member LIF, LIF receptor, and STAT4 drives sustained fibroblast production of inflammatory mediators. *Immunity* **46**, 220–232 (2017).
8. F. Zhang *et al.*, Defining inflammatory cell states in rheumatoid arthritis joint synovial tissues by integrating single-cell transcriptomics and mass cytometry. *Nat. Immunol.* **20**, 928–942 (2019).
9. J. S. Smolen, D. Aletaha, Rheumatoid arthritis therapy reappraisal: Strategies, opportunities and challenges. *Nat. Rev. Rheumatol.* **11**, 276–289 (2015).
10. B. W. Kirkham *et al.*, Synovial membrane cytokine expression is predictive of joint damage progression in rheumatoid arthritis: A two-year prospective study (the DAMAGE study cohort). *Arthritis Rheum.* **54**, 1122–1131 (2006).
11. E. M. Moran *et al.*, Human rheumatoid arthritis tissue production of IL-17A drives matrix and cartilage degradation: Synergy with tumour necrosis factor- α , Oncostatin M and response to biologic therapies. *Arthritis Res. Ther.* **11**, R113 (2009).
12. S. Kotake *et al.*, IL-17 in synovial fluids from patients with rheumatoid arthritis is a potent stimulator of osteoclastogenesis. *J. Clin. Invest.* **103**, 1345–1352 (1999).
13. M. Chabaud, G. Page, P. Miossec, Enhancing effect of IL-1, IL-17, and TNF- α on macrophage inflammatory protein-3 α production in rheumatoid arthritis: Regulation by soluble receptors and Th2 cytokines. *J. Immunol.* **167**, 6015–6020 (2001).
14. F. Fossiez *et al.*, T cell interleukin-17 induces stromal cells to produce proinflammatory and hematopoietic cytokines. *J. Exp. Med.* **183**, 2593–2603 (1996).
15. M. J. Ruddy *et al.*, Functional cooperation between interleukin-17 and tumor necrosis factor- α is mediated by CCAAT/enhancer-binding protein family members. *J. Biol. Chem.* **279**, 2559–2567 (2004).
16. F. Shen, M. J. Ruddy, P. Plamondon, S. L. Gaffen, Cytokines link osteoblasts and inflammation: Microarray analysis of interleukin-17- and TNF- α -induced genes in bone cells. *J. Leukoc. Biol.* **77**, 388–399 (2005).
17. J. Ermann, T. Staton, J. N. Glickman, R. de Waal Malefyt, L. H. Glimcher, Nod/Ripk2 signaling in dendritic cells activates IL-17A-secreting innate lymphoid cells and drives colitis in T-bet $^{-/-}$ -Rag2 $^{-/-}$ (TRUC) mice. *Proc. Natl. Acad. Sci. U.S.A.* **111**, E2559–E2566 (2014).
18. P. J. Koshy *et al.*, Interleukin 17 induces cartilage collagen breakdown: Novel synergistic effects in combination with proinflammatory cytokines. *Ann. Rheum. Dis.* **61**, 704–713 (2002).
19. E. Lubberts, The IL-23-IL-17 axis in inflammatory arthritis. *Nat. Rev. Rheumatol.* **11**, 415–429 (2015).
20. Q. Zhang, M. J. Lenardo, D. Baltimore, 30 years of NF- κ B: A blossoming of relevance to human pathobiology. *Cell* **168**, 37–57 (2017).
21. S. Raychaudhuri, J. M. Stuart, R. B. Altman, Principal components analysis to summarize microarray experiments: Application to sporulation time series. *Pac. Symp. Biocomput.* **38**, 455–466 (2000).
22. A. D. Panopoulos, S. S. Watowich, Granulocyte colony-stimulating factor: Molecular mechanisms of action during steady state and ‘emergency’ hematopoiesis. *Cytokine* **42**, 277–288 (2008).
23. G. Parsonage *et al.*, Prolonged, granulocyte-macrophage colony-stimulating factor-dependent, neutrophil survival following rheumatoid synovial fibroblast activation by IL-17 and TNF α . *Arthritis Res. Ther.* **10**, R47 (2008).
24. H. A. Elshabrawy *et al.*, IL-11 facilitates a novel connection between RA joint fibroblasts and endothelial cells. *Angiogenesis* **21**, 215–228 (2018).
25. K. S. Mix *et al.*, Orphan nuclear receptor NR4A2 induces synovioyte proliferation, invasion, and matrix metalloproteinase 13 transcription. *Arthritis Rheum.* **64**, 2126–2136 (2012).
26. C. M. Aherne *et al.*, Identification of NR4A2 as a transcriptional activator of IL-8 expression in human inflammatory arthritis. *Mol. Immunol.* **46**, 3345–3357 (2009).
27. A. Liberzon *et al.*, The Molecular Signatures Database (MSigDB) hallmark gene set collection. *Cell Syst.* **1**, 417–425 (2015).
28. W. R. Parrish *et al.*, Intra-articular therapy with recombinant human GDF5 arrests disease progression and stimulates cartilage repair in the rat medial meniscus transection (MMT) model of osteoarthritis. *Osteoarthritis Cartilage* **25**, 554–560 (2017).
29. A. J. Roelofs *et al.*, Joint morphogenetic cells in the adult mammalian synovium. *Nat. Commun.* **8**, 15040 (2017).
30. S. Heinz *et al.*, Simple combinations of lineage-determining transcription factors prime cis-regulatory elements required for macrophage and B cell identities. *Mol. Cell* **38**, 576–589 (2010).
31. E. J. Hillmer, H. Zhang, H. S. Li, S. S. Watowich, STAT3 signaling in immunity. *Cytokine Growth Factor Rev.* **31**, 1–15 (2016).
32. G. Nilsen, O. Borgun, K. Liestøl, O. C. Lingjærde, Identifying clusters in genomics data by recursive partitioning. *Stat. Appl. Genet. Mol. Biol.* **12**, 637–652 (2013).
33. A. Fabregat *et al.*, The Reactome Pathway Knowledgebase. *Nucleic Acids Res.* **46**, D649–D655 (2018).
34. A. Khan *et al.*, JASPAR 2018: Update of the open-access database of transcription factor binding profiles and its web framework. *Nucleic Acids Res.* **46**, D260–D266 (2018).
35. Y. Ueda, Y. Su, A. Richmond, CCAAT displacement protein regulates nuclear factor- κ B beta-mediated chemokine transcription in melanoma cells. *Melanoma Res.* **17**, 91–103 (2007).
36. K. Hirota *et al.*, Preferential recruitment of CCR6-expressing Th17 cells to inflamed joints via CCL20 in rheumatoid arthritis and its animal model. *J. Exp. Med.* **204**, 2803–2812 (2007).
37. J. W. Hollingsworth, E. R. Siegel, W. A. Creasey, Granulocyte survival in synovial exudate of patients with rheumatoid arthritis and other inflammatory joint diseases. *Yale J. Biol. Med.* **39**, 289–296 (1967).
38. N. J. Zvaifler, The immunopathology of joint inflammation in rheumatoid arthritis. *Adv. Immunol.* **16**, 265–336 (1973).
39. D. Mulherin, O. Fitzgerald, B. Bresnihan, Synovial tissue macrophage populations and articular damage in rheumatoid arthritis. *Arthritis Rheum.* **39**, 115–124 (1996).
40. J. J. Haringman *et al.*, Synovial tissue macrophages: A sensitive biomarker for response to treatment in patients with rheumatoid arthritis. *Ann. Rheum. Dis.* **64**, 834–838 (2005).
41. Y. Guo *et al.*, CD40L-Dependent pathway is active at various stages of rheumatoid arthritis disease progression. *J. Immunol.* **198**, 4490–4501 (2017).
42. R. Muromoto *et al.*, IL-17A plays a central role in the expression of psoriasis signature genes through the induction of I κ B- ζ in keratinocytes. *Int. Immunol.* **28**, 443–452 (2016).
43. T. Koga *et al.*, Post-transcriptional regulation of IL-6 production by Zc3h12a in fibroblast-like synovial cells. *Clin. Exp. Rheumatol.* **29**, 906–912 (2011).
44. L. Hulea, A. Nepveu, CUX1 transcription factors: From biochemical activities and cell-based assays to mouse models and human diseases. *Gene* **497**, 18–26 (2012).
45. B. Kühnemuth *et al.*, CUX1 modulates polarization of tumor-associated macrophages by antagonizing NF- κ B signaling. *Oncogene* **34**, 177–187 (2015).
46. N. S. Moon *et al.*, S phase-specific proteolytic cleavage is required to activate stable DNA binding by the CDP/Cut homeodomain protein. *Mol. Cell. Biol.* **21**, 6332–6345 (2001).
47. M. Yamamoto *et al.*, Regulation of Toll/IL-1-receptor-mediated gene expression by the inducible nuclear protein I κ B β . *Nature* **430**, 218–222 (2004).
48. S. Yamazaki *et al.*, Gene-specific requirement of a nuclear protein, I κ B β -zeta, for promoter association of inflammatory transcription regulators. *J. Biol. Chem.* **283**, 32404–32411 (2008).
49. R. M. Onishi, S. L. Gaffen, Interleukin-17 and its target genes: Mechanisms of interleukin-17 function in disease. *Immunology* **129**, 311–321 (2010).
50. P. Miossec, Update on interleukin-17: A role in the pathogenesis of inflammatory arthritis and implication for clinical practice. *RMD Open* **3**, e000284 (2017).
51. Y. Hu, F. Shen, N. K. Crellin, W. Ouyang, The IL-17 pathway as a major therapeutic target in autoimmune diseases. *Ann. N. Y. Acad. Sci.* **1217**, 60–76 (2011).
52. R. G. Langley *et al.*; ERASURE Study Group; FIXTURE Study Group, Secukinumab in plaque psoriasis—Results of two phase 3 trials. *N. Engl. J. Med.* **371**, 326–338 (2014).
53. K. B. Gordon *et al.*; UNCOVER-1 Study Group; UNCOVER-2 Study Group; UNCOVER-3 Study Group, Phase 3 trials of ixekizumab in moderate-to-severe plaque psoriasis. *N. Engl. J. Med.* **375**, 345–356 (2016).
54. C.-Q. Chu, D. Swart, D. Alcorn, J. Tocker, K. B. Elkon, Interferon-gamma regulates susceptibility to collagen-induced arthritis through suppression of interleukin-17. *Arthritis Rheum.* **56**, 1145–1151 (2007).
55. P. Miossec, J. K. Kolls, Targeting IL-17 and TH17 cells in chronic inflammation. *Nat. Rev. Drug Discov.* **11**, 763–776 (2012).
56. H. P. Kiener, D. M. Lee, S. K. Agarwal, M. B. Brenner, Cadherin-11 induces rheumatoid arthritis fibroblast-like synoviocytes to form lining layers in vitro. *Am. J. Pathol.* **168**, 1486–1499 (2006).
57. R. A. Irizarry *et al.*, Exploration, normalization, and summaries of high density oligonucleotide array probe level data. *Biostatistics* **4**, 249–264 (2003).
58. M. E. Ritchie *et al.*, Limma powers differential expression analyses for RNA-seq and microarray studies. *Nucleic Acids Res.* **43**, e47 (2015).
59. N. L. Bray, H. Pimentel, P. Melsted, L. Pachter, Near-optimal probabilistic RNA-seq quantification. *Nat. Biotechnol.* **34**, 525–527 (2016).
60. B. L. Aken *et al.*, The Ensembl gene annotation system. *Database (Oxford)* **2016**, baw093 (2016).